

Lasers in Manufacturing Conference 2015

# The role of powder properties on the processability of Aluminium alloys in selective laser melting

Nesma T. Aboulkhair<sup>a,\*</sup>, Ian Maskery<sup>b</sup>, Ian Ashcroft<sup>b</sup>, Chris Tuck<sup>b</sup>, Nicola M. Everitt<sup>a</sup>

<sup>a</sup>Materials, Mechanics and Structures Research Division, Faculty of Engineering, University of Nottingham, Nottingham NG7 2RD, United Kingdom

<sup>b</sup>Manufacturing and Process Technologies Research Division, Faculty of Engineering, University of Nottingham, Nottingham NG7 2RD, United Kingdom

## Abstract

Selective laser melting is used to manufacture complex structures using an additive manufacturing approach with metal powders. It is generally supposed that the quality of the powder plays an important role in the success of the manufacturing process. This is because the powder morphology alongside its size distribution governs the formation of gas pores and controls the flowability. This is important as the process requires successive deposition of uniform layers of powder, which is hindered if the powder does not flow well. In this work, two batches of AlSi10Mg powder with different specifications were characterized in terms of morphology, composition, size distribution, flowability, and apparent density. Bulk samples were created from the powders using selective laser melting and the relative densities were compared. One of the metal powders, which is specially produced for additive manufacturing was found to provide higher quality parts than those fabricated using the other powder, which is not specifically manufactured for that aim. In this paper, we report a successful approach to avoid defects and porosity induced by powder quality by altering the scan strategy, namely scanning each layer twice with different laser powers per scan. The approach could pave the way for successfully overcoming poor quality powder effects.

Keywords: Additive manufacturing; metal powder; selective laser melting; Aluminium; powder characterisation.

## 1. Introduction

Selective laser melting (SLM) is a metal additive manufacturing (AM) process used to fabricate complex parts from loose powders (Frazier, 2014). In subtractive conventional manufacturing, production of a complex structure usually requires a series of manufacturing steps. SLM, being a single step manufacturing technology, drastically shortens production lines, which saves time (Schleifenbaum et al., 2010) and produces minimal waste. In SLM, a layer of powder is deposited onto a powder-bed that a laser beam scans according to information from a sliced and hatched CAD file. After each scan, the piston-controlled powder-bed is lowered and another layer of powder is deposited and scanned. These steps are repeated until the full part is built (Yadroitsev et al., 2007). Based on the process description, SLM is categorized as a powder-based manufacturing process (Gibson et al., 2010).

The process of SLM is controlled by numerous parameters (Gibson et al., 2010), an important one of which is the quality and specifications of the powder (Yadroitsev et al., 2007). The requirement to successively deposit uniform layers of powder dictates particular properties for the powder to enhance its flowability and packing density (Li et al., 2010). These

\* Corresponding author.

E-mail address: emxntab@nottingham.ac.uk.

are mainly governed by the powder morphology and size distribution. In contrast to irregular particles, spherical particles mean better flowability (Yang and Evans, 2007). The presence of gas phases in the starting powder has been asserted to suppress densification during SLM (Dai and Gu, 2014). Li et al. (2010) showed evidence of better densification when using gas atomized stainless steel 316L powder compared to water atomized powder, due to lower oxygen content and higher packing density of the former. Powder used in SLM is not necessarily produced for AM, so the properties of the powder vary largely from one supplier to another. Kempen et al. (2014) compared the morphology and chemical composition of AlSi10Mg from two different suppliers and reported dependency of the resulting samples' relative density on the powder used. However, the morphology of the powder particles in both the batches they used was not particularly spherical and the highest relative density they achieved in their study was 99.4%.

In this paper, the AlSi10Mg powders with different properties, based on the supplier, were used to produce bulk samples via SLM. The quality of the produced parts was examined and related to the variation in the powder's properties. An approach of varying the scanning strategy to remedy defects induced by the powder's poor quality was proposed and validated.

## 2. Experimental Work

Two batches of AlSi10Mg powder from two different suppliers were studied, referred to hereafter as powder (A) and (B). The latter is specially produced for AM to comply with the process requirements. The morphology of the powder was examined using a Philips XL30 scanning electron microscope (SEM) equipped with a secondary electron detector operating at 20 kV. The powder was also cross-sectioned, polished, and imaged using a Nikon Eclipse LV100ND optical microscope. Energy dispersive X-ray diffraction (EDX) served to analyse the chemical composition by means of a detector attached to the SEM. Particle size distribution was analysed using a Malvern Mastersizer 3000. Flowability was tested using the Hall flowmeter funnel following the ASTM standard B213-13 and the apparent density was calculated in accordance with the ASTM standard B212-13.

Cubic samples ( $5 \times 5 \times 5 \text{ mm}^3$ ) were fabricated using a Realizer SLM-50 machine equipped with an yttrium fibre laser (YLM-100-AC). Two sets of samples were produced using the two batches of powder. SLM was conducted under argon to limit contamination and oxidation, with an oxygen level below 0.5%. The build platform was kept at 200 °C to maintain the part at an elevated temperature to avoid deformation by curling due to residual stresses. Samples were processed using a 100 W laser power, 50  $\mu\text{m}$  hatch spacing, 40  $\mu\text{m}$  layer thickness, and a scan speed of 500 mm/s. In each set, half the samples were processed using a uni-directional single scan strategy and the other half was processed using a pre-sinter scan strategy. In the uni-directional single scan strategy, each layer is scanned once, with all scan tracks parallel to the X-axis. In the pre-sinter scan strategy (as defined by Aboulkhair et al., 2014), each layer is scanned twice; the first scan operating at half power (50 W) and the second scan at full power (100 W). The cubic samples were cross-sectioned, polished, and imaged using optical microscopy. The relative density was determined through image processing of optical micrographs using the open source software ImageJ 1.46r (Abramoff et al., 2004).

## 3. Results and Discussion

### 3.1. Powder characterization

The morphology of the powder is shown in Fig. 1. Powder (A) was a mixture of elongated particles and irregularly shaped particles. Powder (B) was largely spherical, which is favoured for SLM requirements. This difference in morphology is expected to grant superiority to powder (B) since the spherical shape allows better flowability and packing density (Li et al., 2010). Some satellites were observed in the micrograph for powder (B) with almost none observed in the examined batch of powder (A). The microstructure of powder (A) – as demonstrated in the cross-section in Fig. 2 (a) – contained Si dendrites. Powder (B)'s microstructure – in Fig. 2 (b) – was a solid solution of cellular  $\alpha$ -Al with Si segregated on the Al grain boundaries. Comparison of the two microstructures indicates that powder (B) cooled faster than (A) during the atomisation process. Minimal inherent porosity was observed in the cross-sections of both powders. Inherent porosity in the powder suggests trapped gases that might promote porosity in processed parts. Gas pores have been previously reported in SLM parts fabricated from AlSi10Mg (Aboulkhair et al., 2014) and attributed to moisture on the powder particle surface as well as gases dissolved in the particles (Weingarten et al., 2015).

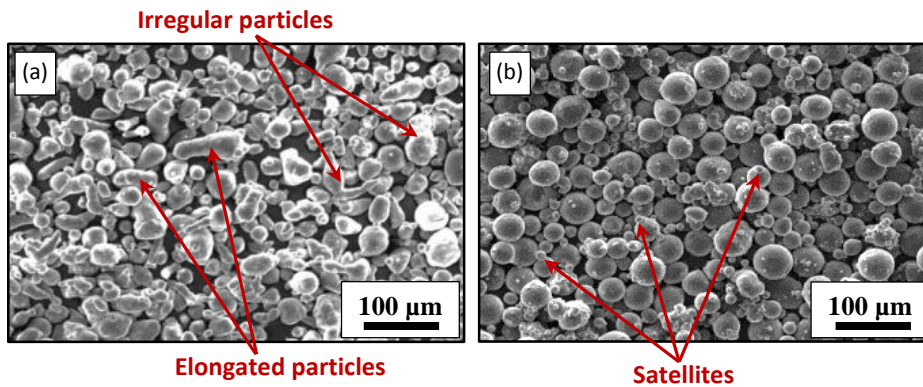


Fig. 1. Morphology of AlSi10Mg powder from batch (a) A and (b) B.

The chemical composition of powder (A) and (B) with respect to the standard composition is listed in Table 1. Powder (A) had Si content within the standard range. Powder (B) on the other hand had higher Si content. The higher Si content in powder (B) makes it a eutectic alloy whereas that of powder (A) is a hypo-eutectic composition (Murray and McAlister, 1984). This difference in Si amount will affect the melting and solidification behaviour during SLM. Higher Si content enhances laser absorption (Kempen et al., 2014), which is beneficial since Al has low absorptivity and high reflectivity compared to other SLM candidate materials (Aboulkhair et al., 2014). In addition, Si increases the metal's fluidity (Haboudou et al., 2003) enhancing its wettability. The drawback of the higher Si content is that it affects the material's mechanical behaviour. Si is added to Al alloys for strengthening, however, in the range close to the eutectic composition it promotes the formation of platelets, which act as sites for crack nucleation under cyclic loading (González et al., 2011), hence reducing the fatigue life. This issue requires investigation, bearing in mind the distinct microstructure developed by selective laser melting (Aboulkhair et al., 2014). The magnesium content is not significantly far off the standard range for both batches of powder (Dadbakhsh and Hao, 2012).

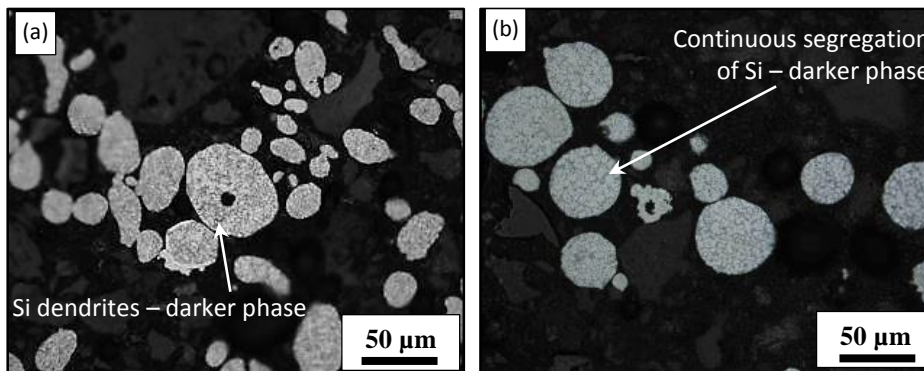


Fig. 2. Microstructure of the cross-sectioned AlSi10Mg powder from batch (a) A and (b) B.

Table 1. Relative chemical composition of AlSi10Mg powders from different suppliers - in weight %.

Powder batch	Mg	Si	Al
(A)	0.48 ± 0.01	11.22 ± 0.19	88.29 ± 0.19
(B)	0.43 ± 0.02	12.36 ± 0.09	87.21 ± 0.11
Standard (Dadbakhsh and Hao, 2012)	0.2 – 0.45	9 - 11	Balance

The particle size distribution in Fig. 3 shows that powder (B) has a more uniform distribution as powder (A) is positively skewed. This skew could be caused by not only the presence of larger particles, but also by the elongated morphology of the particles. The device used for analysis operates by means of measuring the intensity of light scattered as the laser

beam passes through the dispersed particulates. This means that the measurement is influenced by the projected surface of the particle; i.e. particle orientation during data collection will mislead the data for non-spherical particles.

Regarding the powder flowability, powder (A) did not flow through the Hall funnel, indicating poor flowability that cannot be quantified. Poor flowability means that depositing a uniform layer will be challenging during processing. The flow rate of powder (B) was 62 s/50 g. Flowability of a metal powder is governed by its morphology and size distribution and this explains why the flowability of powder (B) was better than powder (A). Powder (A) has an irregular morphology in addition to a skewed particle size distribution. Also, the presence of moisture on the particle's surface would likely contribute to suppressing the powder's flowability. Drying the powder before processing by pre-heating can help overcome this problem in addition to enhancing the powder's laser absorptivity (Yadroitsev et al., 2013). The apparent density of powder (B) was 1.456 g/cm<sup>3</sup>. The apparent density of powder (A) was not determined since the powders did not flow, but lower apparent density is expected because of the irregular morphology of the particles. The better the packing density, the higher the particle contact area, i.e. better consolidation during processing.

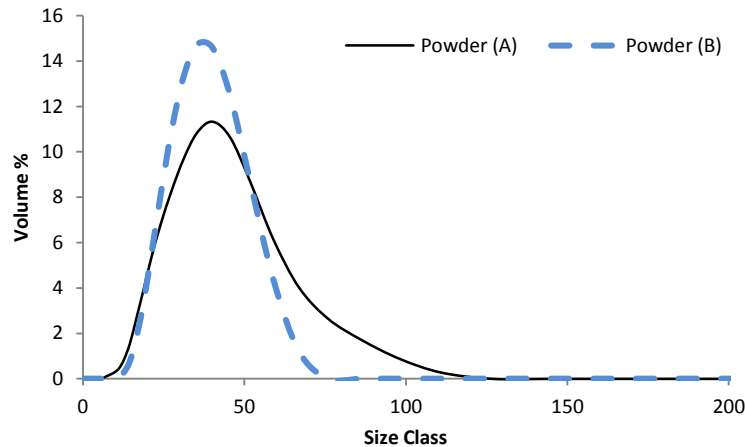


Fig. 3. Particle size distribution for AlSi10Mg powder from supplier (A) and (B).

### 3.2. Effect of powder properties on bulk samples (3D parts) quality

Fig. 4 shows the effect of using different powder (from the same alloy) on the quality of SLM samples. When using the same combination of processing parameters, powder (B) yielded denser parts compared to powder (A). In the single scan strategy, powder (B) showed a relative density of  $(99.62 \pm 0.22)$  % which is an improvement compared to the  $(97.74 \pm 0.09)$  % relative density achieved by using powder (A). These results act as evidence that the properties of the powder used in SLM strongly affect the relative density of the parts produced. Powder (B) surpassed (A) by producing parts of higher relative density and this is attributed to the powder properties and these are:

- The spherical morphology that leads to better flowability (Li et al., 2010) and higher packing and apparent densities
- The particle size distribution that supports better flowability of the powder
- The higher Si content resulting in better laser absorption (Kempen et al., 2014) and smaller difference between the solidus and liquidus temperatures (Bartkowiak et al., 2011)
- The higher Si content enhancing the metal fluidity (Haboudou et al., 2003) as it reduces the metal's surface tension (Shi et al., 2008)

However, it is important to note that the pre-sinter scan strategy, in which each layer is scanned twice with different laser power per scan, has yielded samples with high relative densities using either powder batches. There was no significant difference between the densities of parts from the different powders when using the pre-sinter scan strategy; where powder (A) and (B) yielded samples that were  $(99.77 \pm 0.06)$  % and  $(99.77 \pm 0.07)$  % dense, respectively. It is quite noticeable as well that the standard error was reduced when using the pre-sinter scan strategy, which implies better repeatability of results. This suggests that it is possible to process powder with lower quality – to an extent – or else powder with specifications that do not fully comply with the SLM process requirements without losing the part's quality by means of altering the scan strategy. Powder with poor morphological properties will not allow deposition of a uniform powder layer to be processed by SLM. Thus each layer will suffer defects and irregularities. Sintering the powder in the first scan reduces the chances for defects formation in the full power scan. In this way, defects are remedied, returning a denser layer and consequently a denser part.

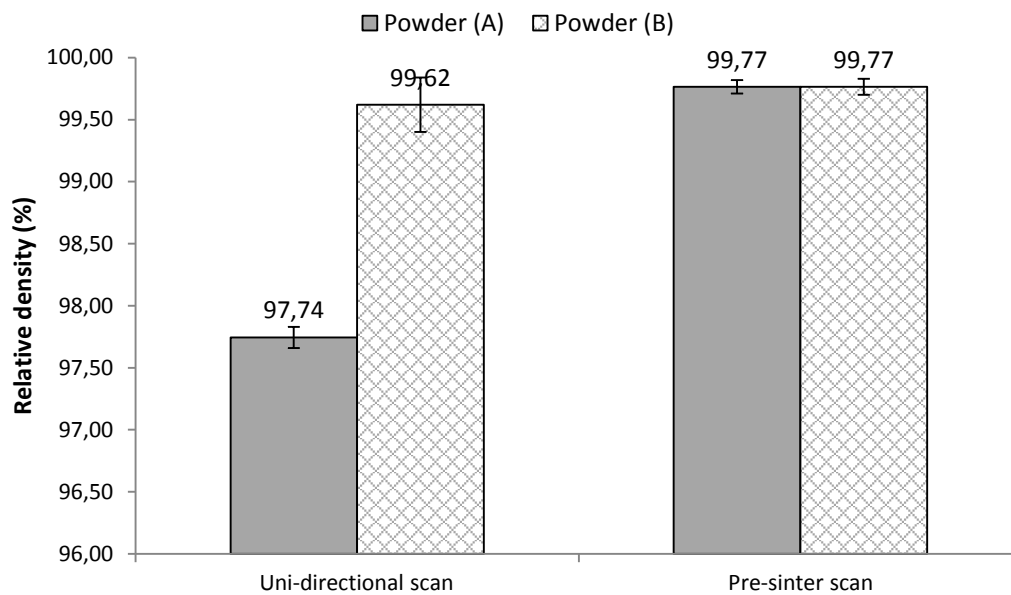


Fig. 4. Relative density of SLM samples processed using different scanning strategies and powders with error bars representing the standard error.

#### 4. Conclusions

This study has demonstrated the variability between the properties and specifications of metal powders from one supplier to another. Attention has to be paid to the specifications of powder to be used in SLM as powder with irregular morphology will not allow proper deposition of a uniform layer of powder. The chemical composition of the powder can alter the melting and solidification behaviour during processing. Although this study has shown that the properties of the powder control the degree of porosity in SLM parts, an approach to reduce porosity using altered scan strategy, using the pre-sinter scan strategy, has proved successful.

#### Acknowledgements

Nesma T. Aboulkhair gratefully acknowledges funding provided by the Dean of Engineering Scholarship for International Research Excellence, Faculty of Engineering, University of Nottingham.

#### References

- Aboulkhair, N.T., Everitt, N.M., Ashcroft, I., Tuck, C., 2014. Reducing porosity in AlSi10Mg parts processed by selective laser melting, *Additive Manufacturing* 1-4, p. 77.
- Abramoff, M. D., Magalhaes, P. J., Ram, S. J., 2004. Image Processing with ImageJ, *Biophotonics International* 11, p. 36.
- ASTM B212-13 Standard Test Method for Apparent Density of Free-Flowing Metal Powders Using the Hall Flowmeter Funnel, ASTM International, West Conshohocken, 2013.
- ASTM B213-13 Standard Test Method for Flow Rate of Free-Flowing Metal Powders Using the Hall Flowmeter Funnel, ASTM International, West Conshohocken, 2013.
- Bartkowiak, K., Ullrich, S., Frick, T., Schmidt, M., 2011. New developments of laser processing aluminium alloys via additive manufacturing technique, *Physics Procedia* 12, p. 393.
- Dadbakhsh, S., and Hao, L., 2012. Effect of Al alloys on selective laser melting behaviour and microstructure of in situ formed particle reinforced composites, *Journal of alloys and compounds* 541, p. 328.
- Dai, D., Gu, D., 2014. Thermal behavior and densification mechanism during selective laser melting of copper matrix composites: Simulation and experiments, *Materials and Design* 55, p. 482.
- Frazier, W.E., 2014. Metal Additive Manufacturing: A Review, *Journal of Materials Engineering and Performance* 23, p. 12.
- Gibson, I., Rosen, W., Stucker, B., 2010. *Additive Manufacturing Technologies*, Springer.
- González, R., Martínez, D. I., González, J., Talamantes, J., Valtierra, S., Colás, R., 2011. Experimental investigation for fatigue strength of a cast Al alloy, *International Journal of Fatigue* 33, p. 273.
- Haboudou, A., Peyre, P., Vannes, A. B., Peix, G., 2003. Reduction of porosity content generated during Nd:YAG laser welding of A356 and AA5083 aluminium alloys, *Materials Science and Engineering A* 363, p. 40.

- Kempen, K., Thijs, L., Van Humbeeck, J., Kruth, J. P., 2014. Processing AlSi10Mg by selective laser melting: parameter optimisation and material characterization, *Materials Science and Technology*.
- Li, R., Shi, Y., Wang, Z., Wang, L., Liu, J., Jiang, W., 2010. Densification behavior of gas and water atomized 316L stainless steel powder during selective laser melting, *Applied Surface Science* 256, p. 4350.
- Murray, J. L., McAlister, A. J., 1984. The Al-Si (Aluminum-Silicon) system, *Bulletin of Alloy Phase Diagrams* 5, p. 74.
- Shi, D., Li, D., Gao, G., 2008. Relation between surface tension and microstructural modification in Al-Si alloys, *Materials Characterization* 59, p. 1541.
- Schleifenbaum, H., Meiners, W., Wissenbach, K., Hinke, C., 2010. Individualized production by means of high power Selective Laser Melting, *CIRP Journal of Manufacturing Science and Technology* 2, p. 161.
- Weingarten, C., Buchbinder, D., Pirch, N., Meiners, W., Wissenbach, K., Poprawe, R., 2015. Formation and reduction of hydrogen porosity during selective laser melting of AlSi10Mg, *Journal of Materials Processing Technology* 221, p. 112.
- Yadroitsev, I., Bertrand, Ph., Smurov, I., 2007. Parametric analysis of the selective laser melting process, *Applied Surface Science* 253, p.8064.
- Yadroitsev, I., Krakhmalev, P., Yadroitsava, I., Johansson, S., Smurov, I., 2013. Energy input effect on morphology and microstructure of selective laser melting single track from metallic powder, *Journal of Materials Processing Technology* 213, p. 606.
- Yang, S., Evans, J. R. G., 2007. Metering and dispensing of powder; the quest for new solid freeforming techniques, *Powder Technology* 178, p. 56.